Pion-capture probabilities in organic molecules

Daphne F. Jackson, C. A. Lewis,* and K. O'Leary

Department of Physics, University of Surrey, Guildford, United Kingdom

(Received 17 September 1981; revised manuscript received 16 February 1982)

Experimental results are presented for atomic-capture probabilities of negative pions in organic molecules. The data are analyzed in terms of atomic and molecular models. This analysis shows that the Fermi-Teller law (Z law) and its modifications do not give an adequate description of the data, but that a mesomolecular model together with hydrogen transfer contains the features essential to fit the data. Clear evidence is given for chemical effects in the pion-capture process.

I. INTRODUCTION

A. Pion interactions in complex materials

The work reported in this paper is part of a program concerned with the interactions of negative pions with complex materials, with particular reference to biological and tissue equivalent materials. We report here the results of experimental studies with a selection of organic molecules, together with a few inorganic molecules, and the analysis of these results in terms of models of the pion-capture process.

A negative-pion incident on any material loses energy initially by ionization. Rather little is known about the next stage of slowing down and adiabatic capture from the continuum into excited states of a pionic atom or molecule.[1] This process is simple only in metals where the pion can give up its energy to the conduction electrons.[2] The deexcitation of an isolated pionic atom occurs by a cascade process initially dominated by nonradiative Auger transitions until the x-ray transitions become most important and circular orbits are populated. The physics of this cascade process in an isolated atom is quite well understood[3] and standard cascade codes[4] are used to calculate the transition rates and x-ray yields for each transition, starting from an initial value of n, which is frequently taken to be $n \sim 16$ where the pion orbit overlaps strongly with the K shell electrons, and from an assumption for the initial distribution of angular momentum states l.

The influence of the medium in which the pionic atom is formed is manifested in a number of ways. Since the binding energy of a pion is proportional to Z^2, a pion captured by hydrogen may be transferred to a more tightly bound orbit around

a nucleus of higher Z. This means that deexcitation of pionic hydrogen $p\pi$ by electromagnetic processes and subsequent nuclear capture of the pion by the proton are in competition with the transfer process,

$$p\pi + Z \rightarrow p + Z\pi .$$
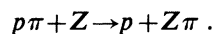
Experimental studies[5,6] have shown that transfer of pions does occur in chemical compounds, mixtures of compounds, and gas mixtures. Chemical and physical effects have been observed[6-8] by measuring the intensities of x-ray lines emitted from selected elements in various compounds and mixtures and comparing the ratios of the summed intensities of a series for the same pair of elements in different samples or by comparing the relative intensities of the lines in a series for the same element in different samples.

A mesomolecular model has been developed by Ponomarev and Schneuwly et al.[9-11] to explain the observed features of pion capture on chemical compounds. Several versions of this model are discussed in Sec. IV B, and in Sec. IV C the model is extended to include transfer from pionic hydrogen.

When a pion reaches the lowest atomic orbits, its distribution overlaps with that of the nucleus. A nuclear interaction can then take place, causing disintegration of the nucleus and emission of short-range charged particles and longer-range neutrons and γ rays.[12] The charged-particle spectra produced from pion interactions in carbon and oxygen are significantly different,[13] although the neutron spectra are quite similar.[14] Since biological tissues consist predominantly of hydrogen, carbon, and oxygen, the emphasis of this work is placed on understanding the process of pion capture in simpler materials consisting of these three elements.

TABLE I. Energies of the pionic Balmer series in carbon, nitrogen, and oxygen.

	Transition	Energy (keV)
Carbon	$3 \rightarrow 2$	18.39
	$4 \rightarrow 2$	24.82
	$5 \rightarrow 2$	27.79
	$6 \rightarrow 2$	29.40
Nitrogen	$3 \rightarrow 2$	25.10
	$4 \rightarrow 2$	33.86
	$5 \rightarrow 2$	37.91
	$6 \rightarrow 2$	40.11
Oxygen	$3 \rightarrow 2$	32.84
	$4 \rightarrow 2$	44.31
	$5 \rightarrow 2$	49.61
	$6 \rightarrow 2$	52.48

B. Outline of this experiment

We have measured the relative intensities of lines in the Balmer series emitted by pionic atoms of carbon and oxygen in a range of samples. For some samples we have also measured the intensities of the Balmer series in nitrogen. It is not feasible to study the pionic Lyman series because of the very considerable broadening of the $1s$ atomic level due to the nuclear absorption of pions from this level. For these light elements the nuclear shifts

TABLE II. Energies of the muonic Lyman series in carbon, nitrogen, and oxygen.

	Transition	Energy (keV)
Carbon	$2 \rightarrow 1$	75.26
	$3 \rightarrow 1$	89.22
	$4 \rightarrow 1$	94.10
	$5 \rightarrow 1$	96.35
	$6 \rightarrow 1$	97.57
Nitrogen	$2 \rightarrow 1$	102.53
	$3 \rightarrow 1$	121.56
	$4 \rightarrow 1$	128.21
	$5 \rightarrow 1$	131.29
	$6 \rightarrow 1$	132.97
Oxygen	$2 \rightarrow 1$	133.95
	$3 \rightarrow 1$	158.85
	$4 \rightarrow 1$	167.55
	$5 \rightarrow 1$	171.58
	$6 \rightarrow 1$	173.77

and widths of the $2p$ and higher levels are negligible[3] and the effect of electron screening is also negligible. It is easy to calculate the energies of the lines and these are given in Tables I and II.

The summed intensities in the Balmer series are taken to be proportional to the total capture probability for a particular element. This assumption is valid if the last few transitions do indeed populate circular orbits and there is relatively little population of the $2s$ level and the higher np states ($n > 2$). For an isolated atom, conventional cascade calculations indicate that this is the case, but if a pionic molecular orbit is formed with high n, the selection rules and the angular momentum distribution at the beginning of the cascade could be changed. We seek first to use the summed intensity ratios to establish whether molecular orbits are formed. Analysis of the intensity variations within the Balmer series for each sample and the consequences for the cascade calculations will be reported later.

We have been able to make a few measurements with muons. In this case we can observe the Lyman series, and the energies of the relevant lines are given in Table II. The summed intensity of the Lyman series will be proportional to the atomic-capture probability provided that there is relatively little population of the $2s$ level.

In pionic atoms there is a possibility of direct nuclear capture on hydrogen of pions in highly excited molecular orbits.[1,10] This means that the probability of transfer to a heavier atom would be reduced in comparison to the transfer in muonic atoms, and hence, in molecules containing hydrogen, the carbon-to-oxygen capture ratio for pions and muons need not be the same. The same comment applies to any other ratio of captures.

II. EXPERIMENTAL PROCEDURE

A. Experimental arrangement

The experiment was performed using the biomedical pion channel[15] at the the Tri-Universities Meson Facility (TRIUMF) Laboratory, Vancouver. For the experiment the channel was tuned to a momentum of 170 ± 10 MeV c^{-1} which, with a beam current of 30 μA, produced an incident flux of approximately 2×10^8 particles s^{-1}. Beam contamination at this momentum amounted to 40% electrons and 5% muons.

A conventional counter telescope, schematically illustrated in Fig. 1, was used to detect pions stopping in the target. It consisted of a triples tele-
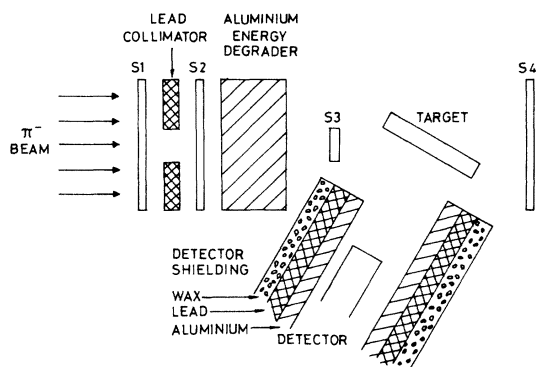
FIG. 1. Schematic diagram of the experimental arrangement.

scope, including a lead collimator, to define the beam incident upon the target which was set in anticoincidence with a high-efficiency counter mounted immediately behind the target. An additional coincidence was set up between the counter telescope and a pion time-of-fight (TOF) signal to reduce false triggers arising from muon or electron stops within the target. To maximize the number of pions stopping in the target, 79 mm of aluminum energy degrader was included between the second and third elements of the telescope. This provided a pion stopping profile within the target with a full width at half maximum (FWHM) of 20 $Kg\,m^{-2}$.

Rectangular targets with dimensions 140×60 $\times10$ mm^3 were mounted at an angle of 30° to the incident beam direction, perpendicular to the x-ray detector axis. In this orientation they presented an area of 60×60 mm^2 to the beam and had an effective thickness of 20 mm. Solid targets were positioned in the beam by clamping them at the base in a small aluminum vice. The remaining targets, mainly powders, were contained within a rectangular aluminum frame with thin (25 μm) aluminum foil beam windows.

Photons emitted from the target were detected using a horizontally mounted hyperpure germanium (HPGe) detector with an active area of diameter 25 mm and active depth of 10 mm situated at a distance of 170 mm from the center of the target. The resolution of this detector was approximately 450 eV at 6 keV and 850 eV at 122 keV. The detector was surrounded by layers of aluminum, lead, and borated wax to provide shielding against x rays emitted from the organic scintillators and fast neutrons. Damage to the detector crystal caused by neutrons emitted from the target could not be avoided, and during the course of the exper-

iment some degradation of the detector resolution was observed, though this did not seriously affect the analysis.

Analog signals from the HPGe detector were accumulated on a 1024-channel analyzer calibrated over the range from 6 to 140 keV. Operation of the analyzer was gated by a suitably delayed coincidence between the pion stop signal from the counter telescope and a fast timing signal from the detector. A gate width of 100 ns was found adequate to collect more than 95% of the detector analog signals corresponding to pion stops.

During typical operation with a proton beam current of 30 μA and using a carbon production target the pion stopping rate was approximately 10^4 counts s^{-1} and the counting rate in the analyzer 10 counts s^{-1}. Spectra were accumulated for approximately 2×10^8 stopping counts and at the termination of each irradiation were written onto floppy disk for subsequent analysis. In addition to the chemical targets, spectra were also obtained from a beryllium target to enable background subtraction to be made.
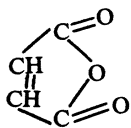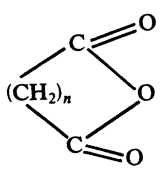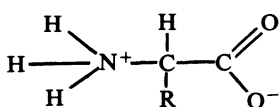
In order to make measurements with muons, some minor changes to the system were required. Specifically, the thickness of energy degrader was increased to 127 mm and the TOF coincidence was adjusted to trigger on muon stops. Because of the higher energy of the muonic x rays the analyzer calibration was extended to cover the range 6—300 keV. Irradiation times were also increased to compensate for the lower proportion of muons in the beam, 5% compared with 55% pions.

B. Choice of targets

Because we are making a relative measurement, i.e., the ratio of captures in two elements, the chosen targets must contain at least two elements other than hydrogen. The emphasis throughout is on the ratio of captures in carbon and oxygen and therefore most of the samples consist of carbon, oxygen, and hydrogen. It was necessary that the materials be available as solid blocks, powders, solids crushable into powders, or exceptionally as stable liquids.

A list of target materials and their chemical composition is given in Table III. The series of dicarboxylic acids was chosen to allow investigation of the role of hydrogen and also because of the biological importance of saturated fatty acids. The cyclic acid anhydrides were chosen to allow comparison of single and double bonds between carbon

TABLE III. Chemical composition of target materials.

(1)	Dicarboxylic acids	COOH $(CH_2)_n$COOH
	Malonic acid	$n=1$
	Succinic acid	$n=2$
	Glutaric acid	$n=3$
	Adipic acid	$n=4$
	Pimelic acid	$n=4$

(2) Cylic acid anhydrides
    Maleic anhydride

Succinic anhydride $n=2$
Glutaric anhydride $n=3$

(3) Saccharides

	$D(+)$ Xylose (pentose)	$C_5H_{10}O_5$
	$D(+)$ Glucose (hexose)	$C_6H_{12}O_6$
	$D(+)$ Mannose (hexose)	$C_6H_{12}O_6$
	Sucrose (disaccharide)	$C_{12}H_{22}O_{11}$
	$D(+)$ Trehalose dihydrate	
	(disaccharide)	$C_{12}H_{22}O_{11} \cdot 2H_2O$

(4) Compounds not containing hydrogen
    Carbon dioxide (dry ice) CO_2 covalent
    Sodium fluoride   NaF ionic

(5) Amino acids

	Glycine	$R=-H$	nonpolar side chain
	DL-α-Alanine	$R=-CH_3$	nonpolar side chain
	DL-Valine	$R=-CH(CH_3)_2$	nonpolar side chain
	L-Serine	$R=-CH_2OH$	polar side chain
	L-Cysteine	$R=-CH_2SH$	polar side chain

(6) Perspex (polymethylmethacrylate) $(C_5H_8O_2)_n$

atoms, and also because there are only CH bonds and no OH bonds in these molecules which may assist in the study of the role of hydrogen. The saccharides were chosen in order to study the effect of increasing the number of atoms whilst the C:O ratio remained constant or nearly so. Since glucose and mannose are structural isomers, comparison of the results for these samples should reveal complex effects due to molecular structure. The saccharides are also important carbohydrates.

The amino acids are an important group of molecules which are essential components of protein molecules. In the cell, the free acids are normally ionized, with the carboxyl group (COOH) losing a hydrogen ion to become negatively charged and the amino group (NH_2) gaining a hydrogen ion to become positively charged. The character of the amino acids is strongly influenced by the side chain, denoted by R. The form of the side chain R for the chosen amino acids is given in Table III. Cer-
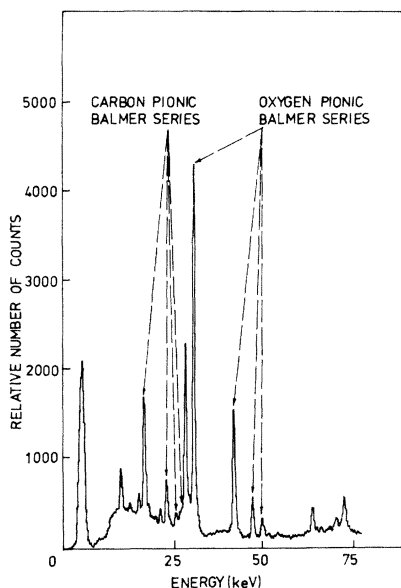
FIG. 2. Typical x-ray spectrum for organic molecules. This example is for malonic acid.

tain of the amino acids and saccharides are strongly lyoluminescent, i.e., they emit light when dissolved after irradiation in the dry state, and this property has potential applications in dosimetry.

The rather difficult measurement with dry ice was attempted because it is important to study a molecule containing carbon and oxygen but no hydrogen. Sodium fluoride was chosen as a simple ionic molecule not containing hydrogen. A number of targets such as water, Be metal, and aluminum were used for calibration purposes.

Part of this experiment was concerned with the potential use of negative pions in radiotherapy, and for this reason several samples of animal tissues

were irradiated and also several materials commonly used as tissue substitutes.[16] The result of these measurements are discussed elsewhere,[17] except those for perspex.

III. ANALYSIS OF DATA AND RESULTS

A. Data analysis

Typical spectra are shown in Fig. 2. Peak areas under the pionic (or muonic) lines were determined from these spectra using a version of the gamma-ray analysis code SAMPO (Ref. 18) which is implemented at the University of London Computer Center. This code uses shape calibration lines obtained from single intense peaks within the spectrum to fit a selected region of the data. Peaks are fitted with Gaussian centroids and exponential tails and the continuum under each peak or set of peaks is fitted with a parabola.

In order to obtain series intensity ratios from the measured peak areas, certain corrections were required, the most important of these being for self-absorption in the target. This correction was formulated by considering the variation of the pion (or muon) stopping profile within the target (assumed to be Gaussian), the solid angle subtended by each element of area in the target to the detector and the attenuation experienced in each ray path within the target. Attenuation coefficients for the targets were obtained by using the mixture rule with elemental attenuation coefficients derived from the recent parametrization by Jackson and Hawkes.[19] The self-absorption correction is given by

$$C = \int_0^{a/2} dx \int_0^b dy \int_0^{c/2} dz \int_0^{d/2} dh \int_{-(d^2/4-h^2)^{1/2}}^{(d^2/4-h^2)^{1/2}} dk \, \exp[\mu_E g\,(x,y,z,h,k)]\exp[-A^2(y-B)^2]\Omega(x,y,z,h,k) \,,$$

where μ_E is the attenuation coefficient at photon energy E,

$$g(x,y,z,h,k) = R(y/L + y) \,,$$

$$\Omega(x,y,z,h,k) = (L + y)/R^3 \,,$$

$$R^2 = (L + y)^2 + (x - h)^2$$

$$+ (z - k)^2 \,,$$

$$B = 0.5b \,(\rho_p/\rho),$$

$$A = 2.041 \,(\rho/\rho_p) \,.$$

In these expressions ρ is the density of the target

and ρ_p is the density of the material in which the stopping profile is measured, (x,y,z) represent the cartesian coordinate system of the target of dimensions $(a \times b \times c)$ with origin at the center, and (h,k) represent the coordinate system of the detector face whose origin was at the center of the face and a distance L from the origin of the target along the axis of the detector.

Detector efficiency corrections were only required in obtaining intensity ratios for the muonic Lyman series which covers the energy range 75—174 keV. In the energy range of interest for the pionic Balmer series, 18—52 keV, the detector

response was found to be constant, within the accuracy of the experimental efficiency measurements. X-ray spectra taken with the beryllium target for both pions and muons indicated that there was no detectable contamination from the organic components in the scintillators.

The principal source of uncertainty in these measurements arose from the determination of peak areas. The main factors influencing the accuracy of these determinations were the peak intensities and the complexity of the region in which the peak or peaks were situated. The percentage errors in the total series intensities, calculated by SAMPO, were generally in the range $3-5\%$ although individual lines within the series showed a wide variation in percentage error from less than 3% for the low Δn transitions. In some specific cases the error in the total series intensity was higher. This occurred, for example, in targets containing nitrogen, when lines of interest, the pionic $4 \rightarrow 2$ line in carbon, and $3 \rightarrow 2$ line in nitrogen were separated by an energy $\Delta E = 280$ eV, less than the detector resolution, and could not be separately resolved by the analysis code. In such cases the combined peak was fitted and the individual intensities estimated on the basis of the intensities of other transitions in the series.

Uncertainties in the self-absorption correction were estimated by evaluating the integral with the mean values of the parameters concerned and also

TABLE IV. Ratio of captures in carbon to oxygen for pions incident on material containing only carbon, oxygen, and hydrogen, or carbon and oxygen.

Material	C:O capture ratio
Malonic acid	0.45 ± 0.03
Succinic acid	0.62 ± 0.03
Glutaric acid	0.83 ± 0.03
Adipic acid	1.17 ± 0.05
Pimelic acid	1.42 ± 0.06
Maleic anhydride	0.79 ± 0.04
Succinic anhydride	0.86 ± 0.04
Glutaric anhydride	1.11 ± 0.05
Xylose	0.57 ± 0.04
Glucose	0.54 ± 0.04
Mannose	0.73 ± 0.04
Sucrose	0.62 ± 0.03
Trehalose dihydrate	0.55 ± 0.03
Carbon dioxide	0.19 ± 0.03
Perspex	1.76 ± 0.07

TABLE V. Ratios of captures in carbon to oxygen and of captures in nitrogen to oxygen for incident pions.

Material	Capture ratio	
	C:O	N:O
Glycine	0.58 ± 0.03	0.42 ± 0.11
Alanine	1.14 ± 0.06	0.53 ± 0.12
Valine	2.07 ± 0.11	0.48 ± 0.10
Serine	0.58 ± 0.04	0.31 ± 0.07
Cysteine	1.05 ± 0.12	0.70 ± 0.20

with one standard deviation added or subtracted from these parameters. This method indicated a percentage error of less than 1% for the correction in almost all cases.

B. Results

The results obtained for the pion capture ratios are given in Tables IV and V. The uncertainties on the N:O capture ratios are quite large for the reasons discussed in the preceding section but the uncertainties on the C:O ratio are a few percent.

For sodium fluoride the ratio of captures in fluorine to captures in sodium is

$$R(Z=9/Z=11)=0.98 \pm 0.15 .$$

Table VI gives the capture ratios derived from the measurements with muons. On the whole, the agreement between our results for pions and muons is not unsatisfactory. A detailed comparison with other muon results for tissue equivalent materials[20] has been given elsewhere.[17]

IV. FORMULAS FOR CAPTURE PROBABILITIES

A. Atomic models

By assuming that the negative pion slows down in a degenerate electron gas, Fermi and Teller[2] de-

TABLE VI. Capture ratios for muons.

Material	C:O capture ratio
Malonic acid	0.49 ± 0.03
Glutaric acid	0.98 ± 0.06
Pimelic acid	1.47 ± 0.10

duced that the relative capture probability on atoms in a compound is proportional to the atomic number Z, i.e.,

$$W(Z) \propto Z , \tag{1}$$

so that for N_i atoms of type Z_i in a molecule the molecular capture probability is given by

$$W(Z_i) = N_i Z_i , \tag{2}$$

and the ratio of capture probabilities in atoms of type Z_1 and Z_2 in the same molecule is

$$R = W(Z_1)/W(Z_2) . \tag{3}$$

A reexamination of the derivation of the Fermi-Teller or Z law leads to the expression[11,21]

$$W(Z) \propto Z^{2/3} . \tag{4}$$

Further analyses along the same lines have led to the formulas

$$W(Z) \propto Z^{1/3} \log(0.57Z) , \tag{5}$$

$$W(Z) \propto Z^{1/3} \log(1.15Z^{1/3})^2 \tag{6}$$

(Refs. 22 and 23, respectively), while the assumption by Petrukhin et al.[24] that the energy loss is proportional to the relative-stopping-power yields the expression

$$W(Z) \propto (Z^{1/3} - 1) . \tag{7}$$

B. Molecular models

In the mesomolecular model, developed by Ponomarev, Schneuwly, and collaborators,[9-11] it is assumed that pions captured by a chemical compound can either be captured directly into atomic orbits or captured initially into molecular orbits lo-cated in the same region as the valence electrons. The simplest expression for the atomic-capture probability of an atom Z_i is then given by[11]

$$W(Z_i) \propto n_i + 2v_i \omega_i , \tag{8}$$

where n_i is the number of core electrons, v_i is the number of valence electrons, and ω_i is the total probability for deexciting from the molecular orbit to an atomic orbit on an atom Z_i.

If the probability of all processes involving the pion in a molecular orbit except deexcitation is represented by $\bar{\omega}$, we have

$$\bar{\omega} + \sum_i \omega_i = 1 . \tag{9}$$

One model of the deexcitation process relevant to nonpolar covalent organic molecules yields[11]

$$\omega_i \propto Z_i^2 \Big/ \sum Z_i^2 . \tag{10}$$

For molecules containing only carbon, oxygen, and hydrogen this model gives $\omega_H \sim 10^{-2}$. If we assume that $\bar{\omega} = 0$ we find

$$\omega_C \simeq 0.36, \quad \omega_O \simeq 0.64, \quad \omega_H \sim 0 . \tag{11}$$

We denote the mesomolecular model with these parameters inserted into Eq. (8) as mesomolecular model A. For the same types of molecules the Z law can be reproduced by inserting into Eq. (8) the values

$$\omega_C = 0.5, \quad \omega_O = 0.5, \quad \omega_H = 0 . \tag{12}$$

Because the electronegativity, which is the power of an atom to attract electrons to itself, is different for different atoms, covalent bonds may have a polar character. In Table VII we give the electronegativity differences for various single bonds and the corresponding percentage ionic character of the

TABLE VII. Electronegativity differences of certain single bonds and percentage ionic character (Ref. 25).

Bond	Electronegativity difference	Percentage ionic character	
C−C	0	0	
O−O	0	0	Nonpolar
C−H	0.4	4	covalent
S−H	0.4	4	bonds
C−N	0.5	6	
N−H	0.9	19	Polar covalent
C−O	1.0	22	bonds
O−H	1.4	39	
Na−F	3.1	91	Ionic bond

bond. Schneuwly *et al.*[11] have suggested that this effect will give rise to localization of the pion in the molecular orbital near to the most electronegative atom. For a bond $Z_1 - Z_2$, the localization probabilities are defined as[11]

$$p_1 = \tfrac{1}{2}(1-\sigma), \quad p_2 = \tfrac{1}{2}(1+\sigma) , \tag{13}$$

where Z_2 is the most electronegative atom and 100σ is the percentage ionic character of the bond. The probability of capture from a mesomolecular orbit to an atomic orbit of atom Z_1 then becomes

$$\omega_1 = p_1 Z_1^2 / (p_1 Z_1^2 + p_2 Z_2^2) . \tag{14}$$

Thus the effect of polarity is to reduce the capture probability for the least electronegative atom and increase it for the most electronegative atom.

In this paper, we are mainly concerned with molecules containing many atoms and hence the description of the polarity of the molecule and the localization of the mesomolecular orbital becomes much more complicated than in the case of a single bond. We will therefore allow ω_C and ω_0 to vary from the values of Eq. (11) and examine the results to see if they are consistent with the prediction of Eq. (14).

C. Hydrogen transfer

A hydrogenic pionic atom can be formed directly or via the molecular orbit. In the first case the capture probability per molecule is proportional to the number of hydrogen atoms multiplied by the atomic number of hydrogen; i.e.,

$$W_D(\mathrm{H}) = N_\mathrm{H} Z_\mathrm{H} , \tag{15}$$

where $Z_\mathrm{H} = 1$ and N_H is the total number of hydrogen atoms in the molecule. In the second case the capture probability is obtained from Eqs. (2) and (8) as

$$W_M(\mathrm{H}) = N_\mathrm{H} \alpha v_\mathrm{H} \omega_\mathrm{H} , \tag{16}$$

where $v_\mathrm{H} = 1$ is the valency and α is a constant believed[10] to lie in the range $1-2$. From our previous discussion, we expect that $\alpha \omega_\mathrm{H} \ll 1$,

$$W_D(\mathrm{H}) \gg W_M(\mathrm{H}) . \tag{17}$$

Because the binding energy of the pion in the atom is proportional to Z^2 the pion bound in a hydrogenic atom may be transferred to a more tightly bound orbit around a nucleus with higher Z. It has been proposed[20] that this transfer takes place

to the nearest-neighboring heavy atom which will normally be the atom to which the hydrogen atom is bonded. Thus the transfer probability T per molecule would be proportional to $\mathrm{H}_i = N_i h_i$, where H_i is the number of hydrogen atoms bonded to an atom of type Z_i. We write the transfer probability per hydrogen bond as $\delta_i a$, where δ_i is the number of electrons participating in the transfer process and a is the probability per electron for transfer from hydrogen to any heavier atom. The total transfer probability per molecule in this nearest-neighbor (NN) model is then given by

$$T_{\mathrm{NN}}(Z_i) = \mathrm{H}_i [W_D(\mathrm{H}) / N_\mathrm{H}] \delta_i a , \tag{18}$$

$$= N_i h_i Z_\mathrm{H} \delta_i a = N_i h_i \delta_i a . \tag{19}$$

We have two extreme pictures of the process which indicate values for δ_i. In the simplest picture the pion is exchanged with one electron in the heavy atom so that

$$\delta_i = 1, \quad \text{for all } i . \tag{20}$$

Alternatively we may envisage a process involving the whole valence cloud, which contains $2v_i - 1$ electrons and one pion, so that

$$\delta_i = 2v_i - 1 . \tag{21}$$

Another possibility is that δ_i might depend on the screened nuclear charge, i.e., $\delta_i = Z_i - n_i = v_i$. This value of δ_i falls between the two extreme cases given by Eqs. (20) and (21).

A different picture of the process arises if we consider the $p\pi$ system as a small neutral object which may detach itself from the original site of the hydrogen atom in the molecule and diffuse through the system. This suggests that the transfer probability per molecule can be written as

$$T_{\mathrm{NO}}(Z_i) = N_i \bar{h}_i \delta_i a , \tag{22}$$

where $\bar{h}_i$ is now some fraction of the total number of hydrogen atoms in the molecule. We do not know how this might depend on Z_i.

D. Total capture ratio in the mesomolecular model with transfer

The ratio per molecule of captures on atoms Z_1 to capture on atoms Z_2 can be obtained from Eqs. (3), (8), and (19) as

$$R = \frac{N_1(n_1 + 2v_1\omega_1 + h_1\delta_1 a)}{N_2(n_2 + 2v_2\omega_2 + h_2\delta_2 a)} . \tag{23}$$
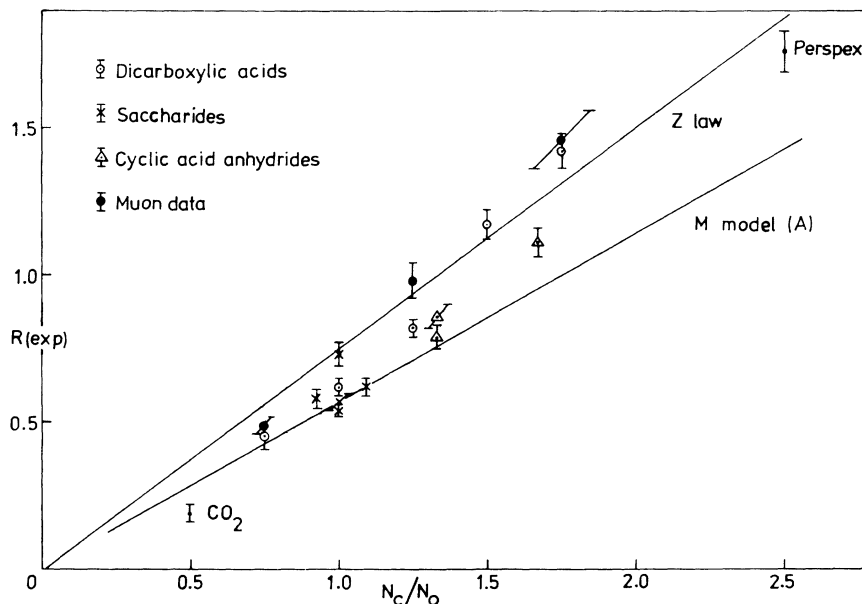
FIG. 3. Experimental results for the C:O atomic-capture ratio R plotted against the ratio $N_C:N_O$ of number of carbon atoms to number of oxygen atoms.

We have used this formula to interpret our data for organic molecules.

If $a=0$ and ω_1, ω_2 are the same for all molecules containing atoms Z_1 and Z_2, Eq. (23) predicts that the relationship between R and N_1/N_2 is a straight line passing through the origin. This will be the case for the Z law and for mesomodel A. However, if hydrogen transfer is important and/or if ω is dependent on molecular structure, discrepancies from a straight line relationship will be seen.

V. DISCUSSION OF THE RESULTS

A. General observations

In Fig. 3 we have plotted the experimental ratio R of captures in carbon to captures in oxygen against the ratio $N_C:N_O$ of the number of carbon atoms to the number of oxygen atoms in each molecule for carbon dioxide, perspex, the saccharides,

the dicarboxylic acids, and the acid anhydrides; i.e., all the materials containing only C, O, and H. It is evident that although the expected trend of increasing capture ratio with increasing $N_C:N_O$ is present, the results do not fall on a single straight line.

The Z law is clearly inadequate. The largest discrepancy is an overestimate of 95% for carbon dioxide. For most, but not all, of the organic molecules the Z law gives discrepancies of 20−25%. The formulas for atomic-capture probabilities which attempt to improve on the Z law do not improve the agreement with the data. This can be seen from Table VIII where we give the relevant values for carbon monoxide and perspex; values for any other molecule can be obtained by adjusting the value of $N_C:N_O$.

The mesomolecular model A is also inadequate and fails for carbon dioxide and perspex. In order to explore the effect of the molecular structure a little more, we have plotted in Fig. 4 the capture

TABLE VIII. Capture ratios predicted by the Z law and modifications of the Z law.

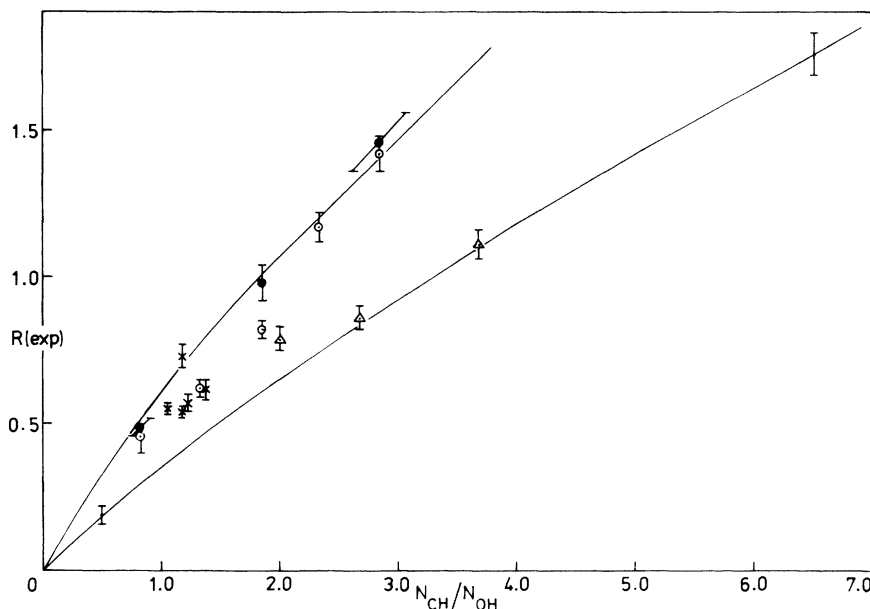|	Z law	Corrected Z law (Ref. 21)	Daniel (Ref. 22)	Vogel *et al.* (Ref. 23)	Petrukhin *et al.* (Ref. 24)
Perspex	1.88	2.06	1.84	2.06	2.12
Carbon dioxide	0.37	0.41	0.37	0.41	0.42

FIG. 4. Experimental results for the C:O atomic-capture ratio R plotted against the ratio N_{CH}:N_{OH} of the number of carbon atoms plus nearest-neighbor hydrogen atoms to the number of oxygen atoms plus nearest-neighbor hydrogen atoms. The symbols are as defined in Fig. 3. The lines are drawn merely to guide the eye.

ratio R against the ratio N_{CH}:N_{OH} where N_{CH} is the number of carbon atoms in the molecule plus the number of hydrogen atoms which are nearest neighbor to carbon, and similarly for N_{OH}. It is already clear from this figure that, if hydrogen transfer is important, the same parameters will not simultaneously describe the higher dicarboxylic acids and the acid anhydrides.

B. Result for carbon dioxide

The result for CO_2 is particularly important because the question of hydrogen transfer does not arise. The Z law and variations of the Z law fail very badly, as can be seen by comparison of Tables IV and VIII. The mesomolecular model A is also unsatisfactory. Using Eq. (23) with $h_C = h_O = 0$ we deduce the best value of ω_C to be

$$\omega_C = 0.19 \pm 0.06 ,   (24)$$

with the restriction that $\omega_C + \omega_O = 1$. This result is very important as it suggests that the relation $\omega \propto Z^2$ may not be generally valid.

The explanation for this result can be found by inserting the value of the ionicity of the carbon-oxygen bond into Eqs. (13) and (14). For a single bond, with $\sigma = 0.22$ from Table VII, we find $p_C = 0.39$, $p_O = 0.61$, and hence $\omega_C = 0.26$. But

since the carbon dioxide molecule contains double bonds it may be more appropriate to take $\sigma = 0.44$, which gives $p_C = 0.28$, $p_O = 0.72$, and hence $\omega_C = 0.21$. Thus the downward shift of ω_C is a clear indication of the influence of the polarity of the bonds and the sensitivity of the atomic-capture ratio to the electronic distribution in the molecule.

C. Result for sodium fluoride

Sodium fluoride is almost completely ionic in character. Thus measurement should therefore serve to confirm the significance of localization of the mesomolecular orbital. The ionicity given in Table VII, inserted in Eqs. (13) and (14), yields a capture ratio of 0.97 while complete ionicity yields a capture ratio of 1.0, both of which are in excellent agreement with the experimental result. The Z law yields the low value of 0.82.

D. Hydrogen transfer

Inclusion of hydrogen transfer is not straightforward because, although we have given in Sec. IV C a number of plausible pictures of the process, there is no quantitative theory which predicts values for the parameters. We concentrate here on the versions of nearest-neighbor transfer.

TABLE IX. Hydrogen-transfer probability a deduced from the pion data.

	$\delta = 1$ $\omega_C = 0.36$	$\delta = 2\nu - 1$ $\omega_C = 0.36$	$\delta = 2\nu - 1$ $\omega_C = 0.23$
Xylose	0	0.00 ± 0.05	0.19 ± 0.06
Glucose	-0.37	-0.04 ± 0.05	0.16 ± 0.05
Mannose	2.42	0.21 ± 0.06	0.44 ± 0.06
Sucrose	0	0.00 ± 0.04	0.19 ± 0.04
Trehalose dihydrate	0.36	0.03 ± 0.05	0.24 ± 0.05
Malonic acid	4.6	0.07 ± 0.07	0.42 ± 0.11
Succinic acid	0.62	0.07 ± 0.04	0.30 ± 0.05
Glutaric acid	0.85	0.10 ± 0.03	0.28 ± 0.04
Adipic acid	1.91	0.22 ± 0.04	0.40 ± 0.04
Pimelic acid	2.00	0.23 ± 0.04	0.40 ± 0.04
Maleic anhydride	0.39	0.06 ± 0.07	0.43 ± 0.09
Succinic anhydride	0.63	0.09 ± 0.05	0.29 ± 0.04
Glutaric anhydride	0.69	0.10 ± 0.03	0.26 ± 0.03
Perspex			0.23 ± 0.02

In Table IX we give the values of the transfer parameter a deduced from the pion data for the molecules containing only C, O, and H for two values of ω_C and with $\omega_C + \omega_O = 1$. These results suggest that the parameter a is quite sensitive to the choice of ω_C and may depend on the molecular structure. In order to examine this point further we have made χ^2 fits to the data, for each group of similar molecules and for the whole set. The parameters were constrained so that $0 \le \omega_C \le 1$, $0 \le \omega_O \le 1$, $0 \le a \le 1$. This procedure yields the following results.

(i) For $\omega_C + \omega_O = 1$, $\delta = 2\nu - 1$. It is not possible to obtain a really good overall fit with two parameters $(\chi^2 \sim 5)$, and taking $a_C \ne a_O$ does not change the overall agreement very much. From Table X it can be seen that the saccharides give $a_C = 0$, $a_C \sim 0.29$, while the acid anhydrides give $a_C \sim 0.13$, and the dicarboxylic acids require large values of both a_C and a_O.

TABLE X. Values of ω_C, a_C, and a_O obtained by fitting the pion and muon data and assuming that $\omega_C + \omega_O = 1$, $\delta = 2\nu - 1$. The first row for each group corresponds to the constraints $\omega_C = 0.25$, $a_C = a_O$, and the second row corresponds to the constraint $a_C = a_O$ with ω_C varied. For the third row, all three parameters are varied.

	ω_C	a_C	a_O	χ^2
Acid anhydrides	0.25	0.258	a	0.98
	0.335	0.130	a	0.00
Dicarboxylic acids	0.25	0.340	0.340	2.90
	0.306	0.256	0.256	2.75
	0.325	0.265	0.513	2.75
Saccharides	0.25	0.192	0.192	4.03
	0.375	0.000	0.000	4.00
	0.415	0.000	0.285	3.98
All the above	0.25	0.266	0.266	5.40
	0.263	0.247	0.247	5.59
	0.290	0.254	0.591	4.85

[a]No transfer occurs to oxygen.

TABLE XI. Values of ω_C deduced from the pion data for fixed values of a and assuming that $\omega_C + \omega_O = 1$.

	a	ω_C
Maleic anhydride	0.25	0.29 ± 0.03
Succinic anhydride	0.25	0.26 ± 0.03
Glutaric anhydride	0.25	0.24 ± 0.03
Malonic acid	0.25	0.28 ± 0.03
Succinic acid	0.25	0.26 ± 0.03
Glutaric acid	0.25	0.25 ± 0.03
Adipic acid	0.25	0.34 ± 0.03
Pimelic acid	0.25	0.35 ± 0.03
Xylose	0	0.36 ± 0.03
Glucose	0	0.33 ± 0.02
Sucrose	0	0.36 ± 0.03
Trehalose dihydrate	0	0.38 ± 0.02
Mannose	0	0.49 ± 0.03
Mannose	0.25	0.34 ± 0.03

(ii) For $\omega_C + \omega_O = 1$, $\delta = 1$. The agreement with all the data is comparable to case (i) but ω_C increases and a or a_C tends to the limiting value of unity. When $a_C \neq a_O$ the dicarboxylic acids and anhydrides require $a_C \lesssim 1.0$, $a_O = 0$, while the saccharides require $a_C = 0$, $a_O \sim 0.5$. In all cases $\omega_C \geq 0.36$ so that this model would not yield agreement with the result for carbon dioxide. If, however, we allow $a > 1$, an overall description can be obtained with a lower value of ω_C. This can be seen from the last line of Table X, where

$\delta_C a_C = \delta_O a_O = 1.77$.

(iii) For $\omega_C = \omega_O = 0.5$. With $\delta = 1$ or $\delta = 2\nu - 1$ and $a_C = a_O$ the values predicted are always above the Z law. It is not possible to fit the acid anhydrides with any variation of $a_C \neq a_O$, but it is possible to fit the saccharides with $\delta = 2\nu - 1$, $a_C = 0$, and $a_O \sim 1.0$.

(iv) For $0.8 \leq (\omega_C + \omega_O) \leq 1$. When we allow $(\omega_C + \omega_O)$ to fall below unity, in order to allow for a significant value of $\omega_H + \bar{\omega}$, there is no significant change in the results for $\delta = 2\nu - 1$. For $\delta = 1$,
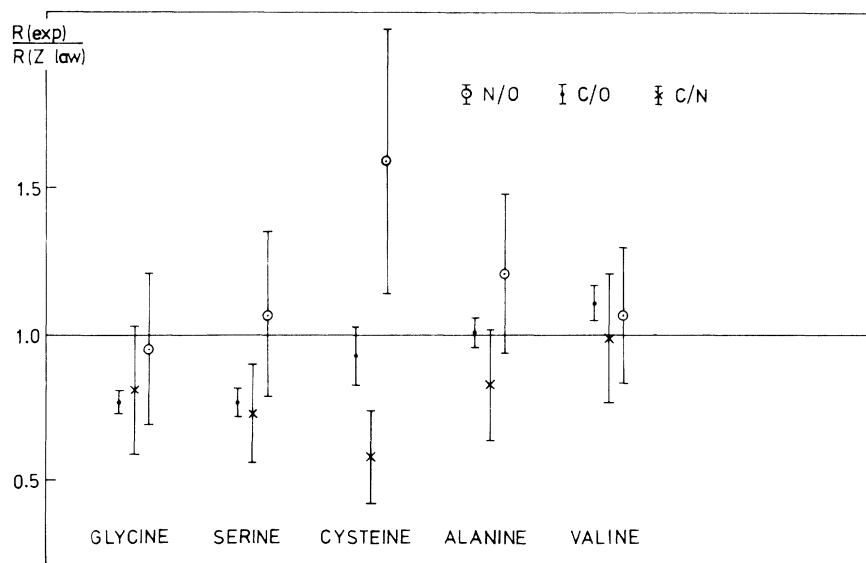

FIG. 5. Experimental results for the C:O, N:O, and C:N capture ratios for the amino acids divided by the theoretical ratio given by the Z law.

TABLE XII. Values of $R(\text{exp})$ divided by $R(\text{theory})$ for capture in carbon and oxygen in the amino acids.

	$R(\text{exp})/R(Z$ law) $\omega_C=0.5, \ a=0$	$R(\text{exp})/R(\text{mesomodel})$ $\omega_C=0.25, \ \omega_O=0.38,$ $\omega_N=0.37$	$R(\text{exp})/R(\text{mesomodel})$ $\omega_C=0.25, \ \omega_O=0.75,$ $\omega_N=0$
Glycine	0.77 ± 0.04	0.85 ± 0.05	0.89 ± 0.05
Serine	0.77 ± 0.05	1.00 ± 0.06	0.92 ± 0.05
Cysteine	0.93 ± 0.10	0.97 ± 0.12	0.98 ± 0.12
Alanine	1.01 ± 0.05	1.04 ± 0.06	1.09 ± 0.06
Valine	1.11 ± 0.06	1.08 ± 0.05	1.06 ± 0.05

$(\omega_C + \omega_O)$ falls to the lower limit for the dicarboxylic acids, while the acid anhydrides show a much smaller fall and the saccharides show a negligible fall. The change occurs primarily in ω_O but the agreement with the data is not significantly improved.

E. Molecular dependence of parameters

It can be seen from Tables IX and X that the parameter a is very sensitive to molecular structure. So far we have assumed that ω_C and ω_O are at least constant for a group of similar molecules and possibly constant for all samples. In Table XI we give the values of ω_C deduced with $\omega_C + \omega_O = 1$ and the values of $a_C = a_O$ indicated from Table X. Again we see a variation through the group of dicarboxylic acids.

F. Results for the amino acids

In Fig. 5 we have plotted the ratios for capture in carbon and oxygen, carbon and nitrogen, and nitrogen and oxygen, divided by the ratios predicted by the Z law. The horizontal axis is used simply to spread out the results, but the ordering of the results does correspond to increasing ratios of carbon-to-nitrogen atoms and carbon-to-oxygen atoms. It is clear that the Z law again fails to fit the data and the discrepancy is most marked in the case of cysteine where there is an extra heavy atom (sulfur).

We have calculated the ratios for capture in carbon and oxygen using the mesomolecular model with the value $\omega_C=0.25$ deduced from the molecules containing only C, O, and H. Quite good agreement with the data is obtained with $\omega_O=0.38$, and $a_C=0.16$, $a_O=0.24$ as can be seen from Table

XII. Using Eq. (9), with $\bar{\omega} + \omega_H=0$, we obtain $\omega_N=0.37$. Using these values of ω_N and ω_O and $a_N=0.066$, we predict N:O capture ratios of 0.48 for glycine, alanine, and valine, and 0.31 for serine; all of these values are in very good agreement with the data as can be seen from Table V. A marginally better fit to the C:O capture ratios is obtained with $\omega_O=0.75$, $a_C=0.27$, $a_O=0.30$, and $\omega_N=0$, $a_N=0.31$. The zero values for a_N or ω_N are presumably related to the ionization of the molecule and reinforce the necessity for a molecular model.

VI. CONCLUSIONS

We have the following.

(a) The Z law and its variations fail to fit the data.

(b) The Z law plus nearest-neighbor transfer also fails to give an overall fit to the data for the molecules containing hydrogen. A subset of the data can be fitted if the transfer takes place only to oxygen atoms.

(c) The mesomolecular model contains an essential feature which makes possible a fit to the data provided that hydrogen transfer is taken into account. This feature is the redistribution of the contribution of the valence electrons, since
$$n_C + 2v_C\omega_C < Z_C \text{ and } n_O + 2v_O\omega_O > Z_O.$$

(d) The probability for atomic capture from the mesomolecular orbit is not proportional to Z^2. The values $\omega_H\sim0$, $\omega_C\sim0.23-0.27$, $\omega_O\sim0.77$ -0.73 appear to give satisfactory overall representation of our data for organic molecules containing only C, O, and H. For the ionic molecule NaF the values $\omega_F\sim0.93$, $\omega_{Na}\sim0.07$ reproduced the capture ratio. It appears that the parameter ω is sensitive to the electronic structure of the molecule in a manner which relates to the localization of the mesomolecular orbital near to atoms of high electronegativity.

(e) Hydrogen transfer is essential to explain our data. The choice $\delta = 2v - 1$ may be preferred, indicating that the whole cloud of valence electrons participates in the transfer process. The transfer parameter a is very sensitive to molecular structure and different parameters for CH and OH bonds may be indicated.

Our overall conclusion is that molecular effects play an important role in pion capture in organic materials. Because these effects are both subtle and complicated, further work is needed to elucidate details of the capture and transfer processes and their influence on the subsequent atomic cascade. Our results should serve as a starting point and guide for further studies.

ACKNOWLEDGMENTS

*Present address: Department of Physics, Mount Vernon Hospital, Northwood, Middlesex, United Kingdom.

[1]S. S. Gershtein and L. I. Ponomarev, in *Muon Physics*, edited by V. W. Hughes and C. S. Wu (Academic, New York, 1975), Vol. III, Chap. VII, Sec. 2.

[2]E. Fermi and E. Teller, Phys. Rev. <u>72</u>, 399 (1947).

[3]R. C. Barrett and D. F. Jackson, *Nuclear Sizes and Structure* (Clarendon, Oxford, 1977), Chaps. 4 and 9.

[4]J. Hüfner, Phys. Lett. C <u>21</u>, 1 (1975); P. K. Haff, P. Vogel, and A. Winther, Phys. Rev. A <u>10</u>, 1430 (1974).

[5]V. I. Petruhkin, V. E. Risin, and V. M. Suvorov, Yad. Fiz. <u>19</u>, 626 (1973) [Sov. J. Nucl. Phys. <u>19</u>, 317 (1974)].

[6]V. I. Petruhkin, V. E. Risin, I. F. Samenkova, and V. M. Suvorov, Zh. Eksp. Teor. Fiz. <u>69</u>, 1883 (1975) [Sov. Phys.—JETP <u>42</u>, 955 (1976)].

[7]L. Tausher, G. Backenstoss, S. Charalambus, H. Daniel, E. Koch, S. Poelz, and H. Schmitt, Phys. Lett. A <u>27</u>, 581 (1968).

[8]G. A. Grin and R. Kunselman, Phys. Lett. B <u>31</u>, 116 (1970).

[9]L. I. Ponomarev, Annu. Rev. Nucl. Sci. <u>23</u>, 395 (1973).

[10]H. Schneuwly, *International School of Physics of Exotic Atoms*, edited by G. Fiorentini and G. Torelli (Servizio Documentazione dei Laboratori Nazionali di Frascati, 1977), p. 255.

[11]H. Schneuwly, V. I. Pokrovsky, and L. I. Ponomarev, Nucl. Phys. A <u>312</u>, 419 (1978).

[12]D. F. Jackson and D. J. Brenner, in *Progress in Particle and Nuclear Physics*, edited by D. H. Wilkinson (Pergamon, Oxford, 1981), Vol. 5, Chap. 4.

[13]U. Klein, Diplomarbeit Universität Karlsruhe, KFK-Report Ext. 3/78-6 (1978); G. Mechtersheimer, G. Büche, U. Klein, W. Kluge, H. Matthäy, D. Münchmeyer, and A. Moline, Phys. Lett. B <u>73</u>, 115 (1978); Nucl. Phys. A <u>324</u>, 379 (1979); D. Münchmeyer, Diplomarbeit Universität Karlsruhe, KFK-Report 2786 B (1979).

[14]U. Klein, G. Büche, W. Kluge, H. Matthäy, G Mechtersheimer, and A. Moline, Nucl. Phys. A <u>329</u>, 339 (1979).

[15]R. M. Henkelman, L. D. Skarsgard, G. K. Y. Lam, R. W. Harrison, and B. Palcic, Int. J. Rad. Oncol. Biol. Phys. <u>2</u>, 123 (1977); R. W. Harrison and D. E. Lobb, IEEE Trans. Nucl. Sci. <u>NS-20</u>, 1029 (1973).

[16]The Hospital Physicists' Association, Scientific Report Series (HPA, London, 1977), p. 20.

[17]C. A. Lewis, K. O'Leary, D. F. Jackson, and G. K. Y. Lam, Phys. Med. Biol. (in press).

[18]J. T. Routti and S. G. Prussin, Nucl. Instrum. Methods <u>72</u>, 125 (1969).

[19]D. F. Jackson and D. J. Hawkes, Phys. Lett. C <u>70</u>, 169 (1981).

[20]J. J. Reidy, R. L. Hutson and K. Springer, IEEE Trans. Nucl. Sci. <u>NS-22</u>, 1780 (1975).

[21]Z. V. Krumshtein, V. I. Petruhkin, L. I. Ponomarev, and Yu D. Prokoshkin, Zh. Eksp. Teor. Fiz. <u>54</u>, 1690 (1968) [Sov. Phys.—JETP <u>27</u>, 906 (1968)].

[22]H. Daniel, Phys. Rev. Lett. <u>35</u>, 1649 (1975).

[23]P. Vogel, P. K. Haff, V. Akylas, and A. Winther, Nucl. Phys A $\underline{254}$, 455 (1975).

[24]V. I. Petruhkin, Yu D. Prokoshkin, and V. M. Suvorov, Zh. Eksp. Teor. Fiz. $\underline{55}$, 2173 (1968) [Sov. Phys.—JETP $\underline{28}$, 1151 (1969)]; V. I. Petruhkin and

V. M. Suvorov, *ibid.* $\underline{70}$, 1145 (1976) [*ibid.* $\underline{43}$, 595 (1976)].

[25]J. G. Stark and H. G. Wallace, Chemistry Data Book (Murray, London, 1971).